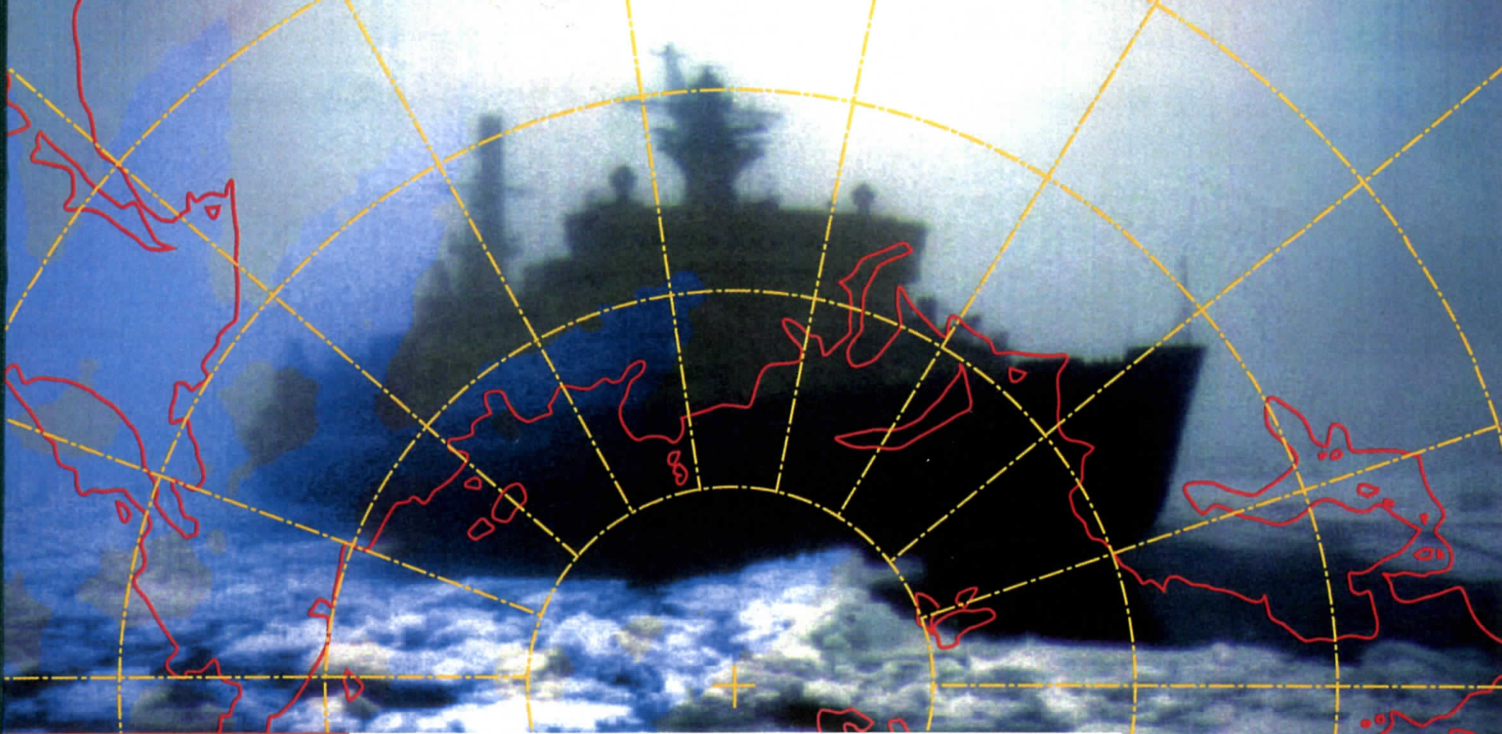

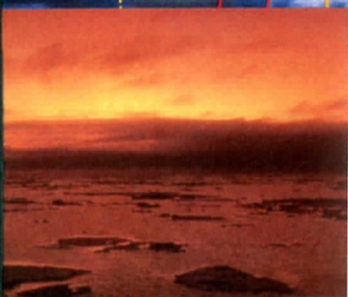

INSROP WORKING PAPER NO. 121 - 1998

The NSR Simulation Study Work Package 2:

Natural Conditions along the Selected Routes

By S. Brestkin, A. Yulin, V. Karklin, I. Ashik, Z. Gudkovich, I. Karelin, S. Klyachkin, E. Makarov, E. Sapershtein, I. Sergeeva, V. Smolyanitsky, K. Teitelbaum and S. Frolov

INSROP International Northern Sea Route Programme

Central Marine Research & Design Institute, Russia

The Fridtjof Nansen Institute, Norway

Ship and Ocean Foundation, Japan

International Northern Sea Route Programme (INSROP)

Central Marine Research & Design Institute, Russia

The Fridtjof Nansen Institute, Norway

Ship & Ocean Foundation, Japan

INSROP WORKING PAPER NO. 121-1998

Box B: The Simulation Study of NSR Commercial Shipping

Work Package 2: Natural Conditions along the Selected Routes

Supervisor: S. Brestkin and A. Yulin, Arctic and Antarctic Research Institute

Title: **Natural Conditions along the Selected Routes**

Authors: **S. Brestkin, A. Yulin, V. Karklin, I. Ashik, Z. Gudkovich, I. Karelin, S. Klyachkin, E. Makarov, E. Sapershtein, I. Sergeeva, V. Smolyanitsky, K. Teitelbaum and S. Frolov**

Address: Arctic and Antarctic Research Institute - AARI
Bering Street 38
199 397 St. Petersburg, Russia

Date: 5 November 1998

Reviewed by: Dr. W. F. Weeks, Portland, Oregon, USA

What is an INSROP Working Paper and how to handle it:

This publication forms part of a Working Paper series from the **International Northern Sea Route Programme - INSROP**. This Working Paper has been evaluated by a reviewer and can be circulated for comments both within and outside the INSROP team, as well as be published in parallel by the researching institution. A Working Paper will in some cases be the final documentation of a technical part of a project, and it can also sometimes be published as part of a more comprehensive INSROP Report. For any comments, please contact the authors of this Working Paper.

FOREWORD - INSROP WORKING PAPER

INSROP is a five-year multidisciplinary and multilateral research programme, the main phase of which commenced in June 1993. The three principal cooperating partners are **Central Marine Research & Design Institute (CNIIMF)**, St. Petersburg, Russia; **Ship and Ocean Foundation (SOF)**, Tokyo, Japan; and **Fridtjof Nansen Institute (FNI)**, Lysaker, Norway. The INSROP Secretariat is shared between CNIIMF and FNI and is located at FNI.

INSROP is split into four main projects: 1) Natural Conditions and Ice Navigation; 2) Environmental Factors; 3) Trade and Commercial Shipping Aspects of the NSR; and 4) Political, Legal and Strategic Factors. The aim of INSROP is to build up a knowledge base adequate to provide a foundation for long-term planning and decision-making by state agencies as well as private companies etc., for purposes of promoting rational decisionmaking concerning the use of the Northern Sea Route for transit and regional development.

INSROP is a direct result of the normalization of the international situation and the Murmansk initiatives of the former Soviet Union in 1987, when the readiness of the USSR to open the NSR for international shipping was officially declared. The Murmansk Initiatives enabled the continuation, expansion and intensification of traditional collaboration between the states in the Arctic, including safety and efficiency of shipping. Russia, being the successor state to the USSR, supports the Murmansk Initiatives. The initiatives stimulated contact and cooperation between CNIIMF and FNI in 1988 and resulted in a pilot study of the NSR in 1991. In 1992 SOF entered INSROP as a third partner on an equal basis with CNIIMF and FNI.

The complete series of publications may be obtained from the Fridtjof Nansen Institute.

SPONSORS OF INSROP

- Nippon Foundation/Ship & Ocean Foundation, Japan
- The government of the Russian Federation
- The Norwegian Research Council
- The Norwegian Ministry of Foreign Affairs
- The Norwegian Ministry of Industry and Energy
- The Norwegian Ministry of the Environment
- The Central and Eastern Europe programme
- State Industry and Regional Development Fund, Norway
- Phillips Petroleum Company, Norway
- Kværner a.s.
- Norwegian Federation of Shipowners
- Norsk Hydro
- Fridtjof Nansen Institute

PROFESSIONAL ORGANISATIONS PERMANENTLY ATTACHED TO INSROP

- Ship & Ocean Foundation, Japan
- Central Marine Research & Design Institute, Russia
- Fridtjof Nansen Institute, Norway
- National Institute of Polar Research, Japan
- Ship Research Institute, Japan
- Murmansk Shipping Company, Russia
- Northern Sea Route Administration, Russia
- Arctic & Antarctic Research Institute, Russia
- Norwegian Polar Research Institute
- SINTEF (Foundation for Scientific and Industrial Research - Civil and Environmental Engineering), Norway.

PROGRAMME COORDINATORS

- **Yuri Ivanov, CNIIMF**
Kavalergardskaya Str.6
St. Petersburg 193015, Russia
Tel: 7 812 271 5633
Fax: 7 812 274 3864
E-mail: cniimf@neva.spb.ru

- **Willy Østreng, FNI**
P.O. Box 326
N-1324 Lysaker, Norway
Tel: 47 67 11 19 00
Fax: 47 67 11 19 10
E-mail: sentralbord@fni.no

- **Hiroyasu Kawai, SOF**
Senpaku Shinko Building
15-16 Toranomon 1-chome
Minato-ku, Tokyo 105-0001, Japan
Tel: 81 3 3502 2371
Fax: 81 3 3502 2033
E-mail: sofkawa@blue.ocn.ne.jp

Introduction

The project aims to describe the natural conditions along two routes of transit navigation selected in Project WP1 (INSROP Phase II). The description will be used for modeling the motion of ships in ice within the framework of Project WP2.

Modeling will be performed by running a model of K. Riska (Lensu et al., 1996), which envisages input of mean monthly (mean seasonal) values of 18 environmental parameters whose list is presented in section 2 of this Report.

The parameters were estimated for 20-mile segments over the period 25 to 40 years by means of calculations on the basis of available data at the AARI permitted for international exchange. In connection with the absence of the calculation methods for some parameters, these methods were developed within the framework of the Project.

The Report consists of three main sections. The first section presents a general description of ice conditions in the Arctic Seas during different seasons of the year. The second section contains an analysis of the influence of different factors on the ship motion speed in ice and a classification of parameters of Riska's model into primary and secondary. The third section describes the initial data used and the methods of calculating the parameters.

1. General description of ice conditions for different seasons of the year

Two main stages of seasonal development of the ice cover are distinguished in the Arctic Seas: autumn-winter (ice conditions and ice growth) and spring-summer (ice melting and decay). At each stage ice conditions of navigation can significantly differ: from easy to heavy and even extreme conditions.

The characteristics of average, heavy and easy ice conditions on different NSR segments separately for each season are given below. From the viewpoint of ice navigation practice, the NSR is not a set of predetermined routes. This notion includes the Siberian shelf seas within which some route or other are selected depending on ice conditions. Hence the general characterization of ice conditions and their classification into types are made in accordance with the regions of the Arctic Seas across which the NSR passes and within which the navigation routes are chosen.

1.1. Ice conditions in the winter season and their classification

1.1.1. Ice formation and growth

Ice formation in the Arctic Seas begins at their northern boundaries among close ice. As a rule, at the end of August stable ice formation begins in the northern East-Siberian Sea, during the first 10-days of September - in the Kara and Laptev Seas and by the end of the second 10-day period of September in the Chukchi Sea. In the coastal shallow regions ice formation begins during the first 10 days of October. On average, the Laptev and the East-Siberian Seas take for 35-40 days to freeze completely and the Kara and the Chukchi Seas take 80-85 days.

Depending on the regional features, the range of variability in the dates of stable ice occurrence in the Arctic Seas vary within 30 to 80 days.

The rate of level ice growth depends on its thickness and differs from region to region. Table 1.1 illustrates the variability in the rates of ice thickness growth. It presents data on the eastern Laptev Sea and the south-western Kara Sea which are distinguished by the largest and least rates.

Table 1.1. Rate of ice growth for different types of conditions in the Arctic Seas from data of polar stations, cm/10-day periods.

Region	Rate of level ice growth	Month							
		X	XI	XII	I	II	III	IY	Y
All seas	high	11.0	12.0	11.5	11.0	8.0	7.0	5.0	3.0
	average	9.5	11.0	10.0	9.0	7.0	6.5	4.0	2.0
	low	6.0	9.0	8.0	7.0	6.0	4.0	2.0	1.0
South-western Kara Sea	high	8.0	10.0	8.5	8.0	7.0	5.5	4.0	3.0
	average	5.0	9.5	8.5	7.5	5.5	4.0	3.0	2.0
	low	0.0	8.0	7.0	6.0	5.0	4.0	3.0	0.0
Eastern Laptev Sea	high	12.5	13.0	12.5	12.0	9.0	8.0	6.0	4.0
	average	11.5	12.5	11.5	11.0	8.0	7.5	5.0	3.0
	low	8.0	10.0	9.0	8.0	7.0	6.5	5.0	2.0

Based on the growth rates, the ice thickness can be calculated for the end of each month (Table 1.2).

Table 1.2. Mean thickness of ice in the regions of the Arctic Seas in the winter season, cm.

Region	Month							
	X	XI	XII	I	II	III	IY	Y
Kara Gate Strait	0	20	44	64	80	98	101	104
South-western Kara Sea	8	37	60	83	102	118	128	134
North-eastern Kara Sea	22	59	87	112	136	156	171	176
Western Laptev Sea	24	61	98	128	148	170	184	192
Eastern Laptev Sea	32	73	110	145	175	195	208	215
Western East-Siberia Sea	30	70	105	136	164	183	196	202
Eastern East-Siberian Sea	28	56	94	126	150	170	184	188
South-western Chukch Sea	22	51	83	110	132	150	160	168
Bering Strait	0	30	80	98	110	133	146	153

1.1.2. Stable formation and development of land fast ice

Stable formation of land fast ice occurs at different time - from the middle of September to early December when ice becomes 10-30 cm thick.

With increasing ice thickness, the boundary of land fast ice extends seaward reaching in February-March its stable position along an isobath of 20-30 m. Near the shores with significant sea depths the fast ice width ranges within 2-4 km to 10-30 km. This is characteristic of the Novaya Zemlya region, Amderma and Yamal coasts, eastern shores of the Severnaya Zemlya archipelago and the region along the Taimyr coast of the Laptev Sea and the Chukchi coast.

In the shallow regions the land fast ice can extend within several tens to several hundreds of kilometers. The land fast ice is most developed in the region of New-Siberian Islands (up to 360 km) and in the western East-Siberian Sea (250 km).

The seaward edge of the fast ice in most regions of the Arctic Seas can be located 10-50 km northward of its average position. The only exception is the western East-Siberian Sea where the northward motion of the fast ice boundary can be 100-140 km.

The minimum fast ice area is observed in the south-western Chukchi Sea and the maximum in the western East-Siberian Sea and the eastern Laptev Sea (Table 1.3).

Table 1.3. Mean and extreme areas of land fast ice in different regions of the Arctic Seas, in percentage of the region area (fig. 1.1).

Region	Minimum area	Mean area	Maximum area
South-western Kara Sea	10	14	26
North-eastern Kara Sea	18	26	33
Western Laptev Sea	17	27	34
Eastern Laptev Sea	42	53	59
Western East-Siberian Sea	23	51	62

Table 1.3. (continued)

Region	Minimum area	Mean area	Maximum area
Eastern East-Siberian Sea	12	21	29
South-western Chukchi Sea	2	6	11

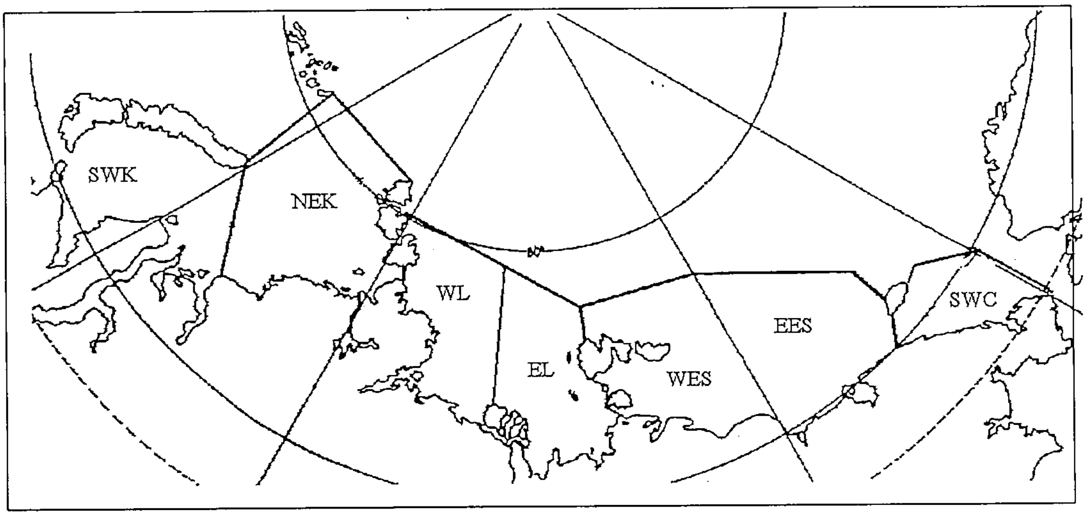

Fig.1.1. The region boundaries of the arctic seas

1.1.3. Drifting ice

In the Kara and Laptev Seas in the autumn and winter seasons ice drifts north-westward contributing to the formation of polynyas. In the East-Siberian Sea the drift is, on average, directed westward making difficult the formation of polynyas. In the Chukchi Sea the drift is directed to the coast during the entire cold period.

The ice drift velocities in most regions of the Arctic Seas in the autumn and winter seasons are close to 6-7 km/day.

Ice of different age categories is present among drifting ice. In the Arctic Seas first-year ice prevails. Old (second-year and multiyear) ice is most often observed in the East-Siberian Sea and in the northern Laptev and Kara Seas. The area occupied by this ice during the autumn and winter seasons does not almost change, on average. Old ice occupies the largest area (about 30%) in the eastern East-Siberian Sea (Table 1.4).

By the end of October young ice prevails in all regions of the Arctic Seas. The area occupied by it varies within 20% (in the south-western Chukchi Sea) to 80% (in the eastern Laptev Sea). This ice is absent in the south-western Kara Sea occupying about 15% of the area in the north-eastern Kara Sea and western Laptev Sea. In the other regions the area occupied by these types of ice is insignificant.

In February all ice age categories are represented in the Arctic Seas. In most regions thick ice prevails occupying 50 to 70% of their water areas. The only exception is the south-western Kara and Chukchi Seas where medium ice prevails.

Table 1.4. Ice age categories in the autumn and winter seasons, in percentage of the area of the regions.

Region	Month														
	X	II	V	X	II	V	X	II	V	X	II	V	X	II	V
	young ice			thin first-year ice			medium first-year ice			thick first-year ice			second-year and multiyear ice		
SWK *	40	12	15	-	35	3	-	53	20	-	-	62	-	-	-
NEK	60	2	6	11	10	5	6	20	5	-	65	81	6	3	3
WL	60	10	8	10	5	3	5	26	8	-	50	73	10	9	8
EL	74	3	7	8	5	3	3	20	4	-	71	86	3	1	-
WES	64	5	4	4	3	2	5	17	2	-	60	80	17	15	12
EES	47	2	2	8	2	1	6	10	2	-	54	65	30	32	30
SWC	24	3	2	5	5	1	-	45	8	-	35	73	8	12	16

At the end of the ice growth period in late May thick first-year ice is predominant everywhere in the Arctic Seas. It occupies 60 to 85% of the area of regions of the Arctic Seas.

1.1.4. Ice age categories and thickness

According to the "International Sea-Ice Nomenclature", each ice age category has a corresponding thickness range:

Young ice	10-30 cm
Thin first-year ice	30-70 cm
Medium first-year ice	70-120 cm
First-year thick ice	120-200 cm
second-year ice and multiyear ice	> 200 cm

The thickness of ice of same age gradations can significantly differ. This is especially true for thick first-year ice. Table 1.5 illustrates thickness distribution taking into account the region and time of the year.

Table 1.5. Mean thickness of thick first-year ice in the regions of the Arctic Seas, cm

Region	Month														
	I			II			III			IY			Y		
	10-day interval														
	I	II	III	I	II	III	I	II	III	I	II	III	I	II	III
SWK	-	-	-	-	-	-	-	-	-	122	125	128	130	132	134
NEK				120	128	136	143	149	156	161	166	171	174	175	176
WL		120	128	135	142	148	156	163	170	175	180	184	187	190	192
EL	122	135	145	155	165	175	182	189	195	200	204	208	211	213	215
WES	120	127	136	146	155	164	171	177	183	188	192	196	198	200	202
EES		120	126	134	142	150	157	164	170	175	180	184	186	187	188
SWC				120	124	132	138	144	150	154	157	160	163	166	168

---

* SWK - south-western Kara Sea; NEK - north-eastern Kara Sea; WL - western Laptev Sea; EL - eastern Laptev Sea; WES - western East-Siberian Sea; EES - eastern East-Siberian Sea; SWC - south-western Chukchi Sea.

As is seen from the table, the thickness of thick first-year ice in the middle of each month varies within the following range:

I	120-135 cm
II	124-165 cm
III	144-189 cm
IV	125-204 cm
V	132-213 cm

1.1.5. Flaw polynyas

Significant in extent (up to hundreds of kilometers) zones with open water or young ice up to 30 cm thick between land fast ice and drifting ice are called flaw polynyas. Table 1.6 presents some characteristics of polynyas in each of the regions of the Arctic Seas.

Table 1.6. Characteristics of flaw polynyas in the regions of the Arctic Seas in March.

Characteristics of flaw polynyas	Region						
	SWK	NEK	WL	EL	WES	EES	SWC
Frequency of occurrence, %	84	87	92	88	79	54	22
Average length, km	609	501	755	388	563	310	300
Maximum length, km	1300	1140	1450	500	990	630	720

1.1.6. Classification of ice conditions by ice thickness

Ice thickness is an integral indicator of severity of the winter season in the Arctic Seas and can characterize the type of ice conditions.

For classification of ice conditions into types, data on ice thickness at the end of the period of growth (third 10-day period) for 1936-1995 were used. In each of the regions of the Arctic Seas ice thickness during the third 10-day period of May was averaged by groups of polar stations located near the Northern Sea Route. Duration of thus obtained series was within 32 to 50 years. Each year for each region belonged to some type or other. The types were identified by means of the following criteria:

Average ice conditions	$H = H_{mean} \pm 0.67\sigma$
Heavy ice conditions	$H_{mean} + 1.2\sigma \geq H > H_{mean} + 0.67\sigma$
Very heavy ice conditions	$H_{max} \geq H > H_{mean} + 1.2\sigma$
Easy ice conditions	$H_{mean} - 0.67\sigma > H \geq H_{mean} - 1.2\sigma$
Very easy ice conditions	$H_{mean} - 1.2\sigma > H \geq H_{min}$

In the presented scale: H_{mean} - mean ice thickness for the entire observation series; H - ice thickness; σ - root-mean square deviation of ice thickness; H_{max} and H_{min} - extreme ice thickness. Table 1.7 presents the results of classification.

As is seen from the table, average conditions prevail in the winter season in the Arctic

Seas, except for the south-western Chukchi Sea. Total frequency of occurrence of heavy and very heavy conditions varies in different regions within 19 to 29% and easy and very easy conditions within 13 to 26%.

Table 1.7. Frequency of occurrence of the types of ice conditions in percentage in the regions of the Arctic Seas and ice thickness ranges corresponding to each type, cm.

Region	Types of ice conditions									
	Average		Heavy		Very heavy		Easy		Very easy	
	Range	Freq-uency	Range	Freq-uency	Range	Freq-uency	Range	Freq-uency	Range	Freq-uency
SWK	134-152	58	153-160	16	161-184	13	126-133	13	-	-
NEK	187-209	54	210-218	14	219-239	10	178-186	10	164-177	12
WL	197-213	56	214-219	6	220-230	13	191-196	9	165-190	16
EL	204-218	64	219-223	18	224-236	3	199-203	3	189-199	12
WES	200-220	58	221-228	14	229-239	10	192-199	6	174-191	12
EES	171-189	53	190-206	21	207-208	2	164-170	16	154-163	8
SWC	163-181	45	182-189	21	190-202	8	155-162	15	135-154	11

1.1.7. Classification of ice conditions in the winter season by the length of polynyas

Classification of ice conditions by types is based on data on the length of polynyas at the end of March during the 1940 to 1995 period. Series of the annual total extent of polynyas in each region of the Arctic Seas were prepared. Conditions of navigation were subdivided into heavy, average and easy as follows:

- heavy conditions if the polynya length was less than 0.5 of its maximum possible length in the region;
- average conditions if the polynya length was more than 0.5 and less than 0.75 of its maximum possible length in the region;
- easy conditions if the polynya length was more than 0.75 of its maximum possible length in the region.

Table 1.8. presents the results of classification.

As is seen from Tables 1.7 and 1.8, heavy types prevail in the regions with a low frequency of occurrence of polynyas. Favorable conditions most often develop in the central regions including the Laptev Sea and the western East-Siberian Sea (total frequency of occurrence of average and easy types is 44-71%). In the Kara Sea same indicator varies within 32-44%.

The maximum total length of flaw polynyas in the Arctic Seas in March (4470 km) was observed in 1995. The maximum possible total length of flaw polynyas is 6730 km. On the whole in the entire flaw polynya zone heavy conditions of navigation prevail (53%), with average type of conditions occurring in 47% of cases. The easy type was not observed at all.

Table 1.8 Frequency of occurrence of the types of ice conditions (%) in the regions of the Arctic Seas and length of polynyas (km) corresponding to each type.

Region	Types of ice conditions					
	Easy		Average		Heavy	
	Length	Frequency	Length	Frequency	Length	Frequency
SWK	≥975	15	651-974	29	<650	56
NEK	≥855	4	571-854	28	<570	68
WL	≥1080	25	721-1079	22	<720	53
EL	≥370	56	251-369	15	<250	29
WES	≥740	15	490-739	29	<490	56
EES	≥470	8	311-469	20	<310	72
SWC	≥500	4	361-499	2	<360	94

1.2. Ice conditions during the summer season and their classification

1.2.1. Ice melt and clearance of the seas

Ice melting in the Arctic Seas begins at different time and falls on the middle of May until the second 10-day period of June. Intensity of melting depends on the dates of the onset of melting. The earlier the ice melt begins, the greater the thickness of melted ice and the sooner the ice disappearance.

At average dates of the onset of melting the level ice thickness (due to melting from the top) can decrease by about 160 cm (see Table 1.9). At early dates of the onset of melting (the second 10-day period of May, on average) ice melts by about 80 cm at the beginning of June and by 180 cm in the first 10-day period of July. At late dates of the onset of melting (end of June) melting is slow ending at the beginning of September. During this time the ice not more than 60-70 cm thick melts out.

Table 1.9. Mean rate of ice melting from the top at the end of a 10-day period of each month at different melting conditions, cm/10-day period.

Month	June			July			August			September		
10-day interval	**I**	**II**	**III**	**I**	**II**	**III**	**I**	**II**	**III**	**I**	**II**	**III**
Average melting conditions	4	20	23	26	23	20	17	13	8	5	1	0
Unfavorable melting conditions	-	-	1	8	15	14	11	7	4	1	-	-
Favorable melting conditions	33	35	33	30	-	-	-	-	-	-	-	-

Under the average conditions of melting all ice age gradations melt out by the end of the summer season, except for thick first-year ice whose thickness decreases up to 20-40 cm, old and also hummocked ice. According to the expedition studies, at the end of September mean ice thickness of 9/10-10/10 in concentration along the shipping routes in different regions is, on average:

South-western Kara Sea	85 cm
North-eastern Kara Sea	105 cm
Western Laptev Sea	105 cm
Eastern Laptev Sea	85 cm
Western East-Siberian Sea	85 cm
Eastern East-Siberian Sea	105 cm
South-western Chukchi Sea	85 cm

The process of sea becoming ice-free is directly connected with melting. The most intense ice disappearance occurs, on average, in August and ends at the end of September (Table 1.10).

Table 1.10. Ice-free area in percentage of the area of the regions (at the end of each month)

Month	Region						
	SWK	NEK	WL	EL	WES	EES	SWC
June	17	0	10	10	0	0	27
July	40	18	24	33	10	6	57
August	85	41	45	69	31	17	75
September	95	53	51	80	49	27	85

1.2.2. Classification of ice conditions during the summer season

During the summer season the ice massifs of the Arctic Seas including ice with concentration of 7/10-10/10 present the main obstacle for navigating the NSR. The most thick of them are the Aion massif (the East-Siberian Sea), the Taimyr ice massif (the Laptev Sea) and the Severo-Zemelsky massif (north-eastern Kara Sea) presenting branches of the oceanic ice massif. These massifs never melt out completely. The Novozemelsky massif (south-western Kara Sea). The Yansky (eastern Laptev Sea) and the Vrangel (south-western Chukchi Sea) ice massifs more often disappear completely at the end of the period of melting. As a rule, the increased areas of the ice massifs create heavy conditions of navigation significantly restricting the possibility for choosing the navigation variants. Vice versa, average and moreover decreased areas of the massifs do nor present significant obstacles for navigation. Hence the classification of summer ice conditions is based on the data of relative area of close ice (Table 1.11).

Table 1.11. Frequency of occurrence of the types of ice conditions (%) in the regions of the Arctic Seas and areas of close ice (% of the region area) corresponding to each type during the summer season.

Region	Types of ice conditions									
	Average		Heavy		Very heavy		Easy		Very easy	
	Area	Frequency	Area	Frequency	Area	Frequency	Area	Frequency	Area	Frequency
SWK	4-20	63	21-26	4	27-45	7	0-3	26	-	-
NEK	31-47	44	32-69	12	70-86	14	9-30	16	1-8	14
WL	33-59	49	60-70	11	70-91	12	22-32	9	8-22	19
EL	5-31	47	32-57	7	57-71	14	0-4	32	-	-
WES	18-50	33	51-63	18	63-87	19	5-17	21	0-4	9
EES	55-75	33	76-83	26	83-91	12	47-54	18	33-46	11
SWC	5-19	44	20-24	12	24-41	9	5-19	35	-	-

For subdividing the summer ice conditions into types, same scale of criteria was used as for ice thickness. The analysis was based on multiyear series of close ice areas (massifs) in August over the 1940-1996 period.

Unfavorable (heavy and very heavy) ice conditions are more often observed in the East-Siberian Sea than in the other regions. Their total frequency of occurrence is 38%. During such years close ice blocks Long and Sannikov Straits. During the entire observation period in 14 cases (24%) heavy and very heavy conditions were formed in these regions simultaneously. In 7 cases (12%) unfavorable conditions were also simultaneously observed in the eastern East-Siberian Sea and in the south-western Chukchi Sea which was usually accompanied by blocking of Long Strait and approaches to it from the west and east.

Heavy and very heavy ice conditions were simultaneously observed in 4-5 regions of the Arctic Seas in 7 cases (12%).

The years when simultaneously in all regions of the Arctic Seas average and easy ice conditions were observed in 14 of 57 cases (24-25%) occur more frequently.

2. Classification of environmental parameters used in Riska's model

2.1. Determination of the influence of these parameters on the ship speed based on the analysis of shipborne ice observational data

The parameters used in Riska's model (Lensu et al., 1996) are connected with the main ice cover characteristics influencing the ship motion speed in the ice. They include:

- ice cover concentration;
- ice thickness (or ice age categories);
- pressure in the ice cover;
- ice forms (horizontal ice floe size);
- hummock and ridge concentration in the ice cover.

2.1.1. Ice concentration and thickness

In the summertime ice conditions of navigation in the Arctic Seas are mainly governed by ice concentration and thickness. The ship motion speed decreases with increasing ice concentration with the speed decrease depending on the ice thickness - the thicker the ice the quicker the speed decrease (Fig. 2.1).

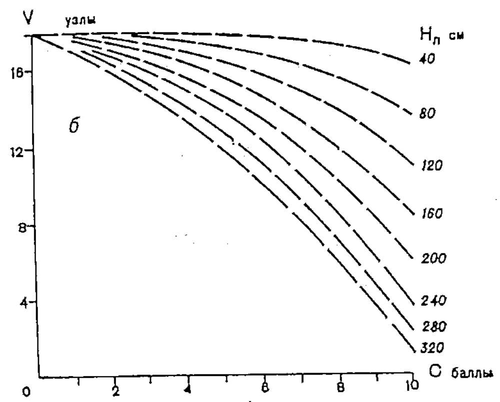

Fig. 2.1. Dependence of the motion speed of the «Arktika» type icebreaker on ice concentration (C) and thickness (H_l) in the summertime (Buzuyev, 1981).

The extent of ice thickness influencing the ship motion speed also depends on the season. Thus at concentration of 10/10 the ship motion speed in level ice in the spring-summer season is much higher as compared to the autumn-winter period (Fig. 2.2). This is connected with the change of ice strength characteristics from winter to summer.

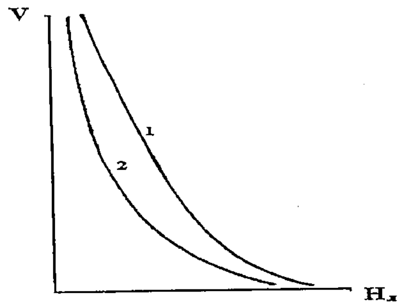

Fig. 2.2. Dependence of the icebreaker motion speed in close ice on ice thickness in spring (1) and autumn (2) Gordiyenko et al., 1967).

In the winter when the Arctic Seas are almost completely ice-covered with concentration of 9/10-10/10, the amount of young ice attains a significant importance.

During the cold season the snow cover depth is a significant navigation characteristic. It was established that the snow cover influence on the ship motion velocity is similar to the ice thickness increase by some value which is proportional to the snow cover depth (Kashtelyan et al., 1968; Svistunov, 1973; Sergeyev, 1979). This parameter is however not taken into account in Riska's model.

2.1.2. Ice pressure in the ice cover

Ice pressure usually occurs at ice concentration of 9/10 and 10/10. It leads to a sharp deterioration of navigation conditions preventing often further ship progress in the ice and causing ice damages.

The influence of ice pressure on the motion velocity usually depends on the type of ship. A dependence between the ship motion velocity and the ice pressure at different ice thickness was established (Gordiyenko et al., 1967) (Fig. 2.3).

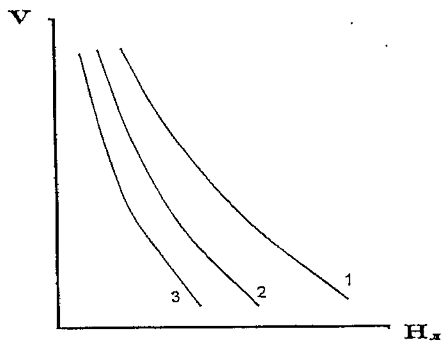

Fig. 2.3. Dependence between the ship motion velocity in the ice with concentration of 9/10-10/10 and the ice thickness in the absence of ice pressure (1), weak pressure (2) and strong pressure (3).

In Riska's model the parameter «pressure» in the ice cover is estimated according to a special scale depending on the direction of wind and currents relative to the coastline. In Russia a principally another approach is used for estimating the degree of ice pressure in the arctic ice (International symbols for sea charts and sea ice nomenclature, 1984). Hence to avoid misunderstanding instead of the «pressure» parameter we estimated its components: «wind direction» and «current direction».

2.1.3. Horizontal dimensions of ice floes (ice forms)

The horizontal dimensions of ice floes have a significant influence on the ship motion velocity (Fig. 2.4).

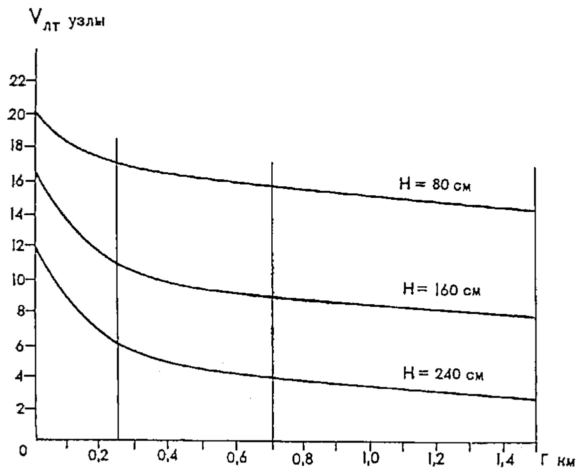

Fig. 2.4. Dependence of the motion velocity of the «Arktika» type icebreaker on the horizontal ice floe dimensions in the summer season at different ice thickness and total concentration of 9/10-10/10 (Buzuyev, 1981).

2.1.4. Hummock and ridge concentration of the ice cover

Hummocked features have a significant influence on the ship motion in ice being sometimes impossible to penetrate. The influence of this factor can be taken into account by determining the so-called equivalent ice thickness. Based on shipborne observations of icebreaker motion (Gordiyenko et al., 1967; Sergeyev and Khromov, 1980), it was found that the motion velocity in level ice of prescribed thickness does not actually differ from the velocity in hummocked ice of same equivalent thickness. The increase in hummock and ridge concentration by 1 conventional unit (Russian national scale, Table 2.1) results in the increment of equivalent ice thickness of 25% .

Table 2.1. The Russian national scale for hummocking

Code figure	**Surface characteristic**	**Hummocked area (% of observed area)**	
		interval	**average**
0	Level ice	0	0
1	Rare hummocked ice	0 - 20	10
2	Level party hummocked ice	20 - 40	30
3	Medium hummocked ice	40 - 60	50
4	Strongly hummocked ice	60 - 80	70
5	Continuous hummocked ice	80 - 100	90

Some pronounced pressure ridges can cause a significant delay in ship progress. Based on shipborne data, a ratio was obtained enabling estimates of transit time connected with overcoming such pressure ridges by the «Arktika» type icebreaker (Buzuyev, 1981):

$$T = \sum^{\mu} 4{,}07 L_T \cdot \frac{h^{0,466}}{\cos \beta},$$

where μ is the number of pressure ridge per unit route, L_T is the pressure ridge width, h is mean ridge height and β is an angle between a normal to the general ridge direction and the ship course.

2.2. Classification of parameters into "primary" and "secondary" depending on their influence on ship motion velocity

For calculations based on the Riska's year round ice navigation model (Lensu et al., 1996), the following parameters are used:

- Cold sum (parameter 1);
- Mean first-year ice concentration (parameter 2);
- Mean multiyear ice concentration (parameter 3);
- Minimum ice concentration (parameter 4);
- Maximum ice concentration (parameter 5);
- Level ice thickness, calculated from the cold sum (parameter 6);
- Mean ice thickness (parameter 7);
- Minimum ice thickness (parameter 8);
- Maximum ice thickness (parameter 9);
- Ice pressure: wind direction (parameter 10), current direction (parameter 11)
- Floe size (parameter 12);
- Mean ridge size (height) (parameter 13);
- Maximum ridge size (parameter 14);
- Maximum possible ridge size (observed/estimated) (parameter 15);
- Mean ridge density (parameter 16);
- Minimum ridge density (parameter 17);
- Maximum ridge density (parameter 18);

The influence of each separate ice cover parameter on the ship speed depends on a set of other parameters. Hence the division of parameters into «primary» and «secondary» is of an arbitrary character.

The influence of different factors on the speed is connected with the tactics of navigation in the ice which depends on the region and the time of the year. Hence the parameters were subdivided separately for the coastal and high-latitudinal routes for the summer and winter seasons of the year (Table 2.2).

In the summertime the «primary parameters» for navigation using both a coastal and a high-latitudinal variants should include ice concentration (parameters 4 and 5) and ice pressure in the ice cover (parameters 10 and 11).

For navigation at high latitudes during the summer one often uses zones within which the ice floes of a small size prevail (Frolov, 1997). Hence for a high-latitudinal route parameter 12 (floe size) should belong to the «primary» parameters.

In the winter when ice concentration in the Arctic Seas is everywhere 9/10-10/10 the parameters connected with ice thickness and age and with ridge density become of utmost importance.

Table 2.2 Primary and secondary ice cover parameters to be used in Riska's model.

Season	Coastal route		High-latitudinal route	
	"Primary" parameters	"Secondary" parameters	"Primary" parameters	"Secondary" parameters
Summer	Minimum concentration	Mean ridge size	Floe size	Mean first-year ice concentration
	Maximum concentration	Maximum ridge size	Minimum concentration	Mean multiyear ice concentration
	Wind direction	Maximum ridge size	Minimum concentration	Cold sum
	Current direction	Mean ridge density	Wind direction	Level ice thickness
		Minimum ridge density	Current direction	Mean ice thickness
		Maximum ridge density		Minimum ice thickness
		Floe size		Maximum ice thickness
		Mean first-year ice concentration		Mean ridge size
		Mean multiyear ice concentration		Maximum ridge size
		Cold sum		Maximum possible ridge size
		Level ice thickness (by the cold sum)		Mean ridge density
		Mean ice thickness		Minimum ridge density
		Minimum ice thickness		Maximum ridge density
		Maximum ice thickness		
Winter	Mean first-year ice concentration	Minimum ice concentration	Floe size	Minimum ice concentration
	Mean multiyear ice concentration	Maximum concentration	Mean first-year ice concentration	Maximum concentration
	Cold sum	Wind direction	Mean multiyear ice concentration	Wind direction
	Level ice thickness (by the cold cum)	Current direction	Cold sum	Current direction
	Mean ice thickness	Floe size	Level ice thickness (by the cold sum)	
	Minimum ice thickness		Mean ice thickness	
	Maximum ice thickness		Minimum ice thickness	
	Mean ridge size		Maximum ice thickness	

Table 2.2 (continued)

Season	Coastal route		High-latitudinal route	
	"Primary" parameters	"Secondary" parameters	"Primary" parameters	"Secondary" parameters
Winter	Maximum ridge size		Mean ridge size	
	Maximum possible ridge size		Maximum ridge size	
	Mean ridge density		Maximum possible ridge size	
	Minimum ridge density		Mean ridge density	
	Maximum ridge density		Minimum ridge density	
			Maximum ridge density	

3. Calculation of parameters used in Riska's model

3.1. Cold sum (parameter 1) and level ice thickness by the cold sum (parameter 6)

For calculating the cold sum (parameter 1) and level ice thickness by the cold sum (parameter 6) data of polar stations on mean air temperature over the 1953 to 1991 period are used. The initial values for calculation were selected from the monthly bulletins for 32 polar stations and were also taken from the charts of mean air temperature for a 10-day period at 18 additional points located near the selected routes. Parameter 1 was calculated for each of 50 points at the end of each month by summing up below zero air temperatures from the time of stable ice formation up to a stable air temperature transfer to above zero temperatures. Parameter 6 was calculated for each of 50 points by a known formula (Zubov, 1945):

$$H^2 + 50H - 8\sum(-t^{\circ}) = 0\,, \qquad (1)$$

where H is the ice thickness calculated by the cold sum - $\sum(-t^{\circ})$

The values of parameters 1 and 6 for each sub-segment of the selected routes were determined by linear interpolation using the most near 3 points.

3.2. Ice concentration (parameters 2 - 5)

The parameters connected with ice concentration were calculated from data on total ice concentration and partial concentration of ice of different age gradations. The initial data sets were obtained by taking the values of total and partial ice concentration from the digital review (generalized for 7-10 days) ice charts (at the points corresponding to the end of each sub-segment). The charts referring to the 1953-1979 period were constructed from data of airborne and satellite ice observations. The charts of the 1990 to 1994 period were plotted from satellite observation data. In all cases data of polar stations, ships and icebreakers were taken into account.

The spatial resolution of initial data is not worse than 4 km. The error in determining the boundaries of uniform ice zones is 2 to 10 km under the normal weather conditions and up to 50 km under the unfavorable conditions. Based on airborne observations, the concentration is determined with an accuracy up to 1/10 and the age category with an accuracy up to 1 age category. If based on satellite observations the accuracy is up to 2/10 and up to 2-3 age categories, respectively.

The accuracy of presenting the ice characteristics in the digital storage formats equals 25 km for the geographical location and 0.5/10 and 1 age category for concentration.

The values of parameters for each sub-segment observed during each month of each year were derived as follows:

- parameter 2 as means of the sum of partial concentrations of new ice, nilas, young and first-year ice;
- parameter 3 as means of the sum of partial concentrations of old, second-year and multiyear ice;
- parameter 4 as a minimum value of total ice concentration;
- parameter 5 as a maximum value of total ice concentration.

3.3. Calculated ice thickness (parameters 7 - 9)

For calculating the parameters connected with the ice thickness the initial data described in section 3.2 were used. For the summer period the data on the ice melting stages over the 1954 to 1986 period were used.

Ice melting stages present a characteristic which was determined during visual airborne observations according to the national scale units (from 0 to 5). The ice melting stage equaling 0, means that melting indications are absent, 5 units mean that ice has strongly decayed and almost disappeared.

The methods for calculating the parameters in the summer and winter differed: the calculations for the summer months (June-September) took into account the thickness decrease due to ice melting. For this purpose an empirical dependence between the relative thickness change in the process of melting - $\Delta H/H$ and the ice melting stage was used – R (Appel, Gudkovich, 1977):

$$R = 11.1 - \frac{10}{0.9025 + 1.02\frac{\Delta H}{H}} \tag{2}$$

From equation (2) the expression for calculating the ice thickness (H_p) can be derived:

$$H_p = H_v - \frac{0.9025RH_v}{11.322 - 1.02R}, \tag{3}$$

here H_V is the ice thickness of a definite age category in May (by the end of the period of growth).

Formula (3) allows taking into account the ice thickness changes due to melting from the top in close ice. With appearance of open water zones among ice the process of melting becomes more rapid due to the heat absorbed by water. For taking this effect into account the following formula was used:

$$H = 0.1[N + (1 - N)k]H_p, \tag{4}$$

where N is ice concentration in tenths; H_p is the ice thickness calculated by formula (3); k is a non-dimensional coefficient (Table 3.1).

Table 3.1. The **k** coefficient values in June-September

Concentration, tenths	June	July	August	September
10	1.0	1.0	1.0	1.0
9	0.975	0.95	0.925	0.90
8	0.95	0.90	0.85	0.80
7	0.925	0.85	0.775	0.70
6	0.90	0.80	0.70	0.60
5	0.875	0.75	0.625	0.50
4	0.85	0.70	0.55	0.40
3	0.825	0.65	0.475	0.30
2	0.80	0.60	0.40	0.20
1	0.775	0.55	0.325	0.10
0	0.75	0.50	0.25	0.00

During the cold period of the year (October-May) the ice thickness of each age category was assumed to be equal to the middle values within the thickness range as indicated in the sea-ice nomenclature (International symbols ...., 1984). The only exception was made for thick first-year ice whose thickness within the sea ice nomenclature range (120 cm-200 cm) was estimated taking into account the data of measurements at polar stations.

After estimating the ice thickness of each age category observed within a sub-segment, the values of parameters were calculated:

- parameter 7 as a weighted thickness mean of all age categories observed taking into account their partial concentration;
- parameter 8 as the least thickness of all age categories observed;
- parameter 9 as the largest thickness of all age categories observed.

3.4. Wind and current direction (parameters 10 - 11)

3.4.1. Calculation of surface wind direction

The calculation of surface wind direction is based on the standard methods. As initial information, the archive of surface atmospheric pressure fields at synoptic times for the 1964 to 1994 period available at the AARI was used ($\Delta\varphi = 5^?$, $\Delta\lambda = 10^?$)

The calculation of surface wind along the sub-segments of the selected routes included 5 stages.

1. Interpolation of atmospheric pressure from the geographical grid points to the rectangular grid points. For this purpose a method of finite elements for tetragonal complex elements was used (Segerlind, 1979). Surface atmospheric pressure was interpolated to the points of the grid covering the Arctic Ocean area (a step $\Delta x = \Delta y$ =30 miles, the X axis is parallel to meridian 40°, the Y axis is parallel to meridian 130°).
2. Calculation of surface wind components at the rectangular grid points. Standard methods are used (Dynamic meteorology, 1976). The surface wind components are calculated by geostrophic wind using the empirical ratios (Ashik, 1995).
3. Averaging the surface wind components over a monthly period.
4. Interpolation of surface wind components to the middles of sub-segments. Similar to Item 1.
5. Calculation of the resulting surface wind direction.

The direction of the resulting wind relative to meridian of the location was determined from the means of surface wind components over a monthly period.

3.4.2. Calculation of the direction of total currents

The total currents in the Arctic Seas are formed under the influence of:

- the wind or wind-driven ice drift on the water surface (drift currents);
- a non-uniform distribution of the pressure forces (gradient currents);
- tidal forces (tidal currents).

The contribution of tidal currents to the total current can be neglected due to their periodical character. The gradient currents are governed, on the one hand, by the non-uniform distribution of atmospheric pressure and surge distortions of the level surface and on the other hand, by a non-uniform density field resulting from non-uniform temperature and salinity fields (density currents). That is, for calculating the total currents it is necessary to take into account the atmospheric pressure, wind stress at the water surface and spatial distribution of water temperature and salinity.

The area of the Arctic Ocean is insufficiently covered with information on the spatial temperature and salinity distribution to estimate mean current speed for every month of the year. The variability of the density fields of water of the Arctic Ocean is comparatively small. Hence it can be suggested that the use of mean multiyear values of water temperature and salinity for calculating the density currents will not result in significant errors.

For calculating the field of density currents a widespread dynamic method was employed (Zubov, 1947). The calculation of wind-driven currents was performed by means of a modified Davies's model (Davies, 1981).

The calculation of total currents included the following 5 stages:

1. Based on mean multiyear data on sea water temperature and salinity distribution for the summer and winter seasons and using a dynamic method, the components of the density current vectors were calculated.
2. Based on the available archive of surface atmospheric pressure fields and using a three-dimensional barotropic model of ice and ocean dynamics the components of wind-driven current components were calculated.
3. By means of algebraic summation of the density and wind-driven current components the components of total currents were calculated.
4. The components of total currents were interpolated to the middles of sub-segments of the selected routes.
5. Based on the total current components, its direction was calculated relative to meridian of location.

3.5. Floe size (parameter 12)

The calculation of the prevailing size of the ice floes is based on the data of visual airborne observations of ice floe size distribution (Shilnikov, 1973). The ice floe size distribution is estimated using a scale of 10 units (A handbook..., 1981; International symbols for sea charts and sea ice nomenclature, 1984). These observations were carried out during the 1954 to 1985 period from February to August. In connection with an irregular character of these observations the data are available only in 30% of cases. In the absence of observation data the prevailing floe size can be estimated on the basis of statistical relations with other characteristics.

In the wintertime (October-May) the ice floe size distribution (P) changes from 0 to 5 units and is estimated by a distance between the cracks and leads.

Floe size distribution (P), conventional units	0	1	2	3	4	5
Distance between cracks, km	no	> 10	5-10	3-5	2-3	< 2

The prevailing ice floe size (km) was determined over the winter months on the basis of data on floe size distribution using an empirical formula (Borodachev, 1974):

$$L = \frac{50}{1 + 1.85\boldsymbol{P} + 0.7\boldsymbol{P}^2} \quad (5)$$

In the summer (June-September) the ice floe size distribution (P) changes from 5 to 10 units and is estimated by a relative area of the ice floes with a size of more than 0.5 km from 0.1-0.5 km and less than (<0.1 km). In the event the observation data are absent, the ice floe size distribution in the summer can be determined with sufficient accuracy by empirical formula (Appel, Gudkovich, 1977):

$$\boldsymbol{P} = 6.5 - 0.15N + R, \quad (6)$$

where N is ice concentration $(0 \leq N \leq 10)$, R is the ice stage of melting $(0 \leq R \leq 5)$.

For estimating a typical floe size during this period the integral functions of ice floe size distribution can be used (Gorbunov, Timokhov, 1974):

$$\boldsymbol{\Phi}(r) = \frac{1}{(r_m)^2}(r - r_m)^2, \quad (7)$$

here r_m is the maximum ice floe size (m) which is connected with the P value (Russian national scale) by a ratio (Appel, Gudkovich, 1977):

$$r_m = 50\boldsymbol{P}^2 - 1200\boldsymbol{P} + 7000 \quad (8)$$

Assuming for the most typical ice floe size ?(r) = 0.5 (this means that 50% of the area of the ice cover is occupied by ice floes with a size r_m and more), the prevailing ice floe size (km) can be determined using formulas (7) and (8):

$$L = 0.0006 r_m$$

3.6. Ridge size (height) (parameters 13 - 15)

During the entire period of studies of the Arctic Ocean only fragmentary and occasional observations of the ridge height were carried out.

First reliable data on the ridge height in the Arctic were reported by Vrangel (1838) and later by Makarov (1901) and Kolchak (1909). According to Kolchak, the usual ridge height is 4-6 m. Especially large ridges up to 8 m are noted at the land fast ice boundary.

From current sources it is known that the mean height of pressure ridges is 1.6 to 1.9 m among first-year ice and 2.0 to 2.5 m in multiyear ice (Gavrilo et al., 1974).

Vast evidence on the ridge height in the Arctic Basin and the marginal seas was collected by Romanov (1991) at numerous aircraft landings on the ice during the 1972 to 1981 period. According to his data, the ridge height decreases, on average, from the northern shores of the Canadian Arctic archipelago (3-3.2 m) towards the shores of Siberia (0.8-1 m).

The maximum ridge height reaches 3 m in the Barents and Kara Seas , 4-5 m in the north of these seas and 1-5 m in the East-Siberian and Laptev Seas: 1-3 m in first-year ice and 3.1-5.5 m in multiyear ice (Romanov, 1991).

In some cases data on mean multiyear ridge height might be insufficient. The required information on the mean and maximum ridge height for different seasons and regions can be obtained on the basis of statistics and a probability theory. For this purpose one can use the relations between the ridge height and other ice cover characteristics which were either observed on a regular basis or reliably calculated.

3.6.1. Determination of mean ridge height (parameter 13)

Mean ridge height H_S in the regions of the Arctic Basin and the marginal seas was calculated on the basis of data (Romanov, 1991) on mean ice thickness h_S and the ratio of the mean ridge height to the thickness of ambient level ice (Table 1). The four lower lines of the table contain data of shipborne observations (Frolov, pesonal communication).

Table 3.2. Mean ice thickness h_S, the ratio H_S/h_S and mean ridge height H_S

Region	**h_S, cm**	**H_S/h_S**	**H_S, cm**
Northern Barents Sea	145	0.86	125
South-western Kara Sea	120	1.10	132
Kara Sea	148	0.93	138
Western Laptev Sea	184	0.99	182
Laptev Sea	157	0.98	154
East-Siberian Sea	213	0.89	190
Chukchi Sea	155	1.11	172
Beaufort Sea	334	0.65	217
Arctic Basin (near the pole)	310	0.77	239
Arctic Basin (north of the Siberian coast and Vrangel Island)	241	0.86	207
Kara Sea (land fast ice)	180	0.68	122
Laptev Sea (land fast ice)	195	0.64	125
East-Siberian Sea (land fast ice)	206	0.67	138
Pechora Sea	45	1.55	70
Zhelaniya Cape region	112	1.00	112
Vilkitsky Strait (land fast ice)	176	0.70	124
North-eastern Kara Sea (land fast ice)	168	0.55	93

As follows from the analysis of Table 3.2 there is a noticeable linear relation between the mean ridge height and mean thickness of ambient level ice. These relations significantly differ for land fast ice and drifting ice (Fig. 3.1).

This dependence can be represented in the analytical form by the following formula, according to which parameter 13 was calculated for each sub-segment:

$$H_s = nh_s^m \qquad (9)$$

H_S and h_S are expressed in cm, the parameters m and n are determined by the least squares method:

- for drifting ice m = 0.62, n = 6.59
- for land fast ice m = 0.94, n = 0.88

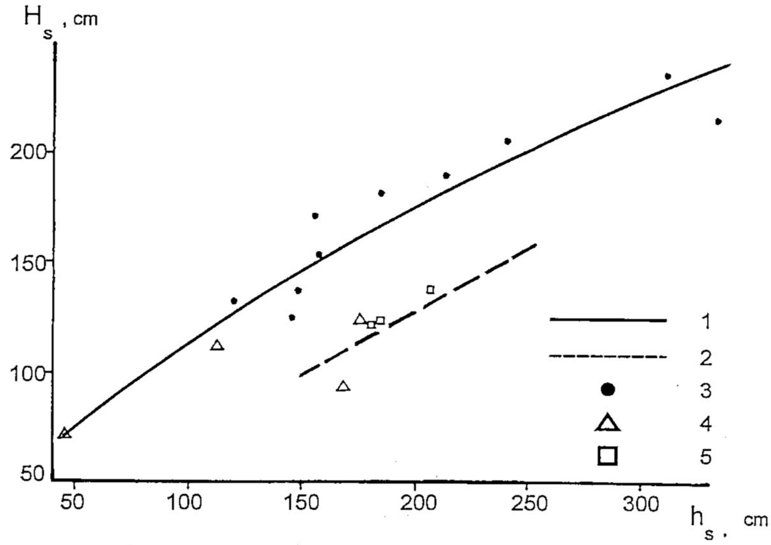

Fig. 3.1. Dependence of mean ridge height (H_S) on the ice thickness (h_S) (1 - for drifting ice; 2 - for land fast ice; 3 - for drifting ice from Romanov's data; 4 - for drifting ice from Frolov's data; 5 - for land fast ice from Frolov's data)

3.6.2. Determination of the maximum ridge height (parameters 14 and 15).

The maximum ridge height can be determined as a random value whose excess can occur with a small prescribed probability. The distribution function F(H) will express the probability that the random value H (ridge height) is equal to or more than some prescribed value (H_m):

$$F(H) = P(H \geq H_m) \tag{10}$$

The study of ridge distribution was performed by a group of US scientists (Hibler, et al., 1972) and later by Wadhams (1977). As shown by the results of ridge height estimates, both distributions satisfy the criterion χ^2 at a 95% confidence level. However, they give significant errors for the ridge heights of more than 3 m (Tucker, 1979 et al., Kreider, Thro, 1981). The parameters of the distribution functions according to Hibler et al. and to Wadhams, depend not only on the mean value but also on the assumed threshold ridge height value. The introduction of threshold values is connected with the method of measurements and results in the distortion of the form of the distribution function since it cuts off its part referring to the values below the threshold. Russian observations contain data on the ridge height without introducing the threshold values.

The Weibull's integral distribution function (1951) is quite a convenient approximation of expression (10). It was used for describing the distribution and estimating the maximum wind speed values (Anapolskaya, Gandin, 1958) and the ice drift velocity (Gudkovich et al., 1989). The expression of this formula is written as:

$$P(H \geq H_m) = \exp\left[-\delta (H/H_s)^\gamma\right], \tag{11}$$

where H_S is the mean value of H; δ, γ are the empirical parameters.

By raising both parts of equality (11) to the power of (-1) and taking a two-fold logarithm, we obtain:

$$\ln[\ln(1/P)] = \ln\delta + \gamma \ln(H/H_s) \tag{12}$$

This function is convenient to depict in the rectified and superposed coordinate grid: in the abscissa axis ln(H/H_S) is plotted and in the ordinate axis a double logarithm of 1/P (Fig. 3.2.). Then the dependence (12) will be expressed by a direct line of the form:

$$y = \gamma x + b, \tag{13}$$

where $y = \ln[\ln(1/P)]$,

$x = \ln(H/H_s)$,

$b = \ln\delta$

For determining the parameters of the Weibull's ridge height distribution function the data in (Romanov, 1991; Gavrilo et al., 1974) were used, as well as data of ridge height measurements from icebreakers submitted by Frolov (personal communication).

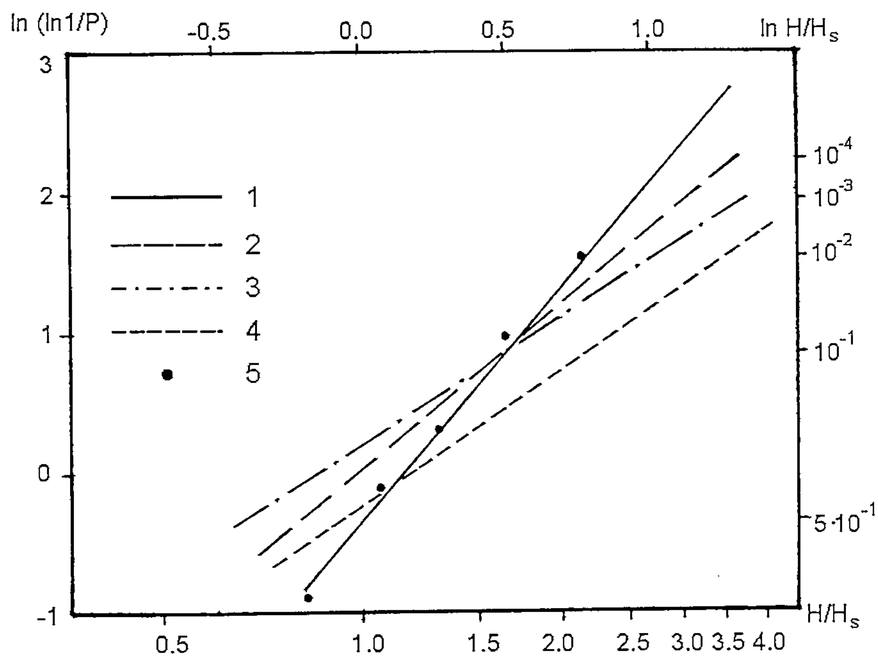

Fig. 3.2. Weibull's distribution functions of the ridge height

(1 - adopted from Romanov; 2 - first-year ice of the Arctic Basin adopted from Gavrilo et al.; 3 - multiyear ice of the Arctic Basin adopted from Gavrilo et al.; 4 - land fast ice adopted from Frolov; 5 - adopted from Romanov).

The parameters .γ.. and .δ.. are easily found graphically or by the least squares method. The order for their calculation based on the frequency of occurrence of different gradations of the investigated values is described in detail in (Gudkovich et al., 1989).

Table 3.3. presents the Weibull's distribution parameters derived by the least squares method for multiyear and first-year ice.

Table 3.3. Weibulls's distribution parameters of the ridge height for different ice types

Region	Ice cover characteristics	Mean ice thickness (cm)	Weibull's parameters	
			γ	δ
Arctic Basin	multiyear ice	203	1.30	1.22
Arctic Basin	thick first-year ice	161	1.68	1.04
Kara Sea (near Zhelaniya cape)	medium first-year ice	112	3.40	0.67
Pechora Sea	thin first-year ice	45	2.32	0.77
Vilkitsky Strait	land fast ice	176	1.46	0.76
Kara Sea	land fast ice	168	1.34	0.79

By using data of Table 3.3 the dependence of Weibull's parameters on the mean ice thickness can be approximated graphically (Fig. 3.3).

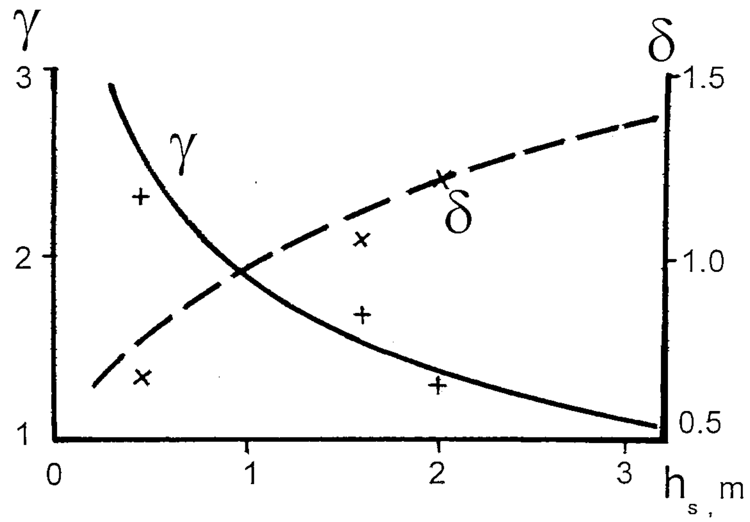

Fig. 3.3. Dependence of the Weibull's parameters on mean ice thickness (+, × - observed data)

For calculations it is convenient to use an analytical representation of the Weibull's parameters:

$$\gamma = -0.67 \ln h_s + 1.85 \qquad (14)$$

$$\delta = 0.97 h_s^{0.31} \qquad (15)$$

Here, the ice thickness h_S is expressed in meters.

Thus for estimating the maximum ridge height of the prescribed probability it is necessary to know the mean ridge height. This value is usually calculated more reliably.

For each sub-segment of the selected routes the maximum ridge height (cm) was calculated as a value which can be exceeded with a probability of 1% ($H_{0.01}$- parameter 14) and 0.1% ($H_{0.001}$ - parameter 15)

$$H_{0.01} = [\exp(\ln(\ln 100) + \gamma \ln H_s - \ln \delta)] \qquad (16)$$

$$H_{0.001} = [\exp(\ln(\ln 1000) + \gamma \ln H_s - \ln \delta)] \qquad (17)$$

3.7. Ridge density (parameters 16 – 18)

The initial data for calculating the ridge density (the number of encounters with ridges per 1 km route) are the mean ridge height (parameter 13) and hummock and ridge concentration (the area covered with ridges according to a scale of 1 to 5 units). The following calculation algorithm was used.

A relative ridge area (corresponds to a relative route length in hummocked ice) is determined according to formula (Bushuyev, Loschilov, 1967):

$$S_T = 0.047T^{4/3}, \tag{18}$$

where S_T is a relative area in unit fractions, T is hummock and ridge concentration in conventional units.

The width of the ridge base (B_S) is connected with its height (H_S) by ratio (Gavrilo, Grischenko, Loschilov, 1974):

$$B_s = 5H_s \tag{19}$$

It follows from (18) and (19) that the number of ridges per 1 km route (ridge density) D equals:

$$D = \frac{47T^{4/3}}{5H_s} \tag{20}$$

The values of parameters were derived as follows:

- parameter 16 as a mean ridge density observed within a sub-segment during each month of each year;
- parameter 17 as a minimum ridge density observed within a sub-segment during each month of each year;
- parameter 18 as a maximum ridge density observed within the sub-segment during each month of each year.

References

A handbook on airborne ice reconnaissance, 1981, Leningrad, 240 p.

Anapolskaya L.Ye., Gandin L.S., 1958. Methods of determining the calculated wind speeds, Moscow, Meteorology and Hydrology, No. 10, p.10.

Appel I.L., Gudkovich Z.M., 1977. Taking into account the influence of thermal processes on the change in concentration of the ice cover. Proc./AARI, v. 346, p. 29-44.

Ashik I.M.,1995. Numerical Predicdition of Sea Surges and Ice Conditions in the Laptev and East Siberian Sea, Berichte zur Polarforschung, Heft Nr. 176/1995, p. 47–54.

Borodachev V.Ye., 1974. On the block structure of the ice cover, Proc./AARI, v. 316, p. 25-27.

Bushuyev A.V., Loschilov V.S., 1967. The accuracy of airborne observations and mapping of sea ice, Proc./AARI, v. 257, p. 84-92.

Buzuyev A.Ya., 1981: Influence of natural conditions on shipping in the ice-infested seas, Leningrad, Gidrometeoizdat, 1981, 200 p.

Buzuyev A.Ya., Fedyakov V.Ye., 1981. Variability of ice conditions along the ship navigation route, Moscow, Meteorology and Hydrology, N 2, p. 69-76.

Buzuyev A.Ya., Gordiyenko P.A., 1976. A quantitative estimate of the difficulty of ice navigation, Moscow, Meteorology and hydrology, No. 9, p. 60-66.

Davies A.M., 1981. Three-dimensional modelling of surges, Flood due to high winds and tides, Ed. D.H.Peregrine, p. 45–75.

Dynamic meteorology, 1976. Leningrad, 607 p.

Frolov S.V., 1997. Ice Conditions of Navigation in the Central Arctic Ocean// Proceedings of the 16-th International Conference on OMAE, ASME. New York. - 1997. Vol. IV, - P. 401-406.

Gavrilo V.P., Grischenko V.D., Loschilov V.S., 1974. To the question of full-scale studies of morphology of ridges on the Arctic ice and the possibility of modeling the processes of ridging, Proc./AARI, v. 316, p. 70-76.

Gorbunov Yu.A., Timokhov L.A., 1974. Variability of the ice floe size distribution, Proc./AARI, v. 316, p.89-95.

Gordiyenko P.A., Buzuyev A.Ya., Sergeyev G.N., 1967. Study of the sea ice cover as a shipping medium, Leningrad, problems of the Arctic and the Antarctic, N 27, p. 93-104.

Gudkovich Z.M., Kirillov A.A., Kovalev Ye.G., Smetannikova A.V., Spichkin V.A., 1972. Grounds of the methods of long-range ice forecasts for the Arctic Seas, Leningrad, 348 p.

Gudkovich Z.M., Voinov G.N., Losev S.M., 1989. To the methods of calculating the maximum ice drift velocities, In: Regime-forming factors, information base and methods of its analysis, Leningrad, p. 232-237.

Hibler W.D., Weeks W.F., Mock S.J., 1972. Statistical Aspects of sea-ice Ridge Distribution, Journ. of Geophys. Res., vol. 77, N 30, p. 5954-5970.

International symbols for sea charts and sea ice nomenclature. 1984, Leningrad, 56 p.

Kashtelyan V.I., Poznyak I.I., Ryvlin A.Ya., 1968. Ice resistance to ship motion, Leningrad Sudostroyeniye, 238 p.

Kolchak A.V., 1909. Ice of the Kara and Siberian Seas, St. Petersburg, 170 p.

Kreider J.R., Thro M.E., 1981. Statistical techniques for analyses of sea ice pressure ridge distribution, POAC-81, 6-th Intern. Conf. on Port and Ocean Engineering, vol. 2, p. 789-798.

Lensu ?., Heale S., Riska K., Kujala P., 1996. Ice environment and ship hull loading along the NSR. Vol. 66 – 1996. INSROP working paper I.1.10, 118 p.

Makarov S.O., 1901. The «Yermak» in ice, St. Petersburg, 507 p.

Romanov I.P., 1991. Ice cover of the Arctic Basin, Leningrad, 212 p.

Segerlind L., 1979. Application of the finite elements methods, Moscow, 286 p.

Sergeyev G.N., 1978. Use of data on ice thickness for assessing navigability of ice routes by ships, Leningrad, problems of the Arctic and the Antarctic, N 54, p. 54-56.

Sergeyev G.N., Khromov Yu.N., 1980. Hummock and ridge concentration and ice resistance to moving ship, Moscow, Meteorology and Hydrology, N 10, p. 100-104.

Shilnikov V.I., 1973. On the methods of observations of ice floe distribution in the ice cover, Proc./AARI, v. 307, p. 187-193.

Tucker W.B., Weeks W.F., Frank M., 1979. Sea Ice Ridging over the Alaskan continental Shelf, Journ. of Geophys. Res., vol. 84, NC8, p. 4885-4897.

Vrangel F.P., 1838. A historical overview of voyages in the Arctic Ocean between the Kara Sea and Bering Strait up to 1820, St. Petersburg, 120 p.

Wadhams P. A., 1977. Comparison of Sonar and Laser Profiles along corresponding Tracks in Arctic Ocean, AIDJEX/ICSI Symposium: Sea Ice Processes and Models, University of Washington Press, p. 283-299.

Weibull W., 1951. A statistical distribution function with a wide application area, Journ. Of Applied Mechanics, v. 18, N.3.

Zubov N.N., 1945. Ice of the Arctic, Moscow, 360 p.

Zubov N.N., 1947. Dynamic oceanology, Leningrad, 430 p.

4 August 1998

Review of "Natural Conditions Along the Selected Routes" by Brestkin, Yulin, et al.

Review prepared for INSROP by W. F. Weeks, Ph.D., Glaciologist

General
I find this paper to be generally well written and understandable. However a careful critique by your inhouse editor would clearly be useful. The paper is quite informative in that it describes the environmental conditions that will serve as input to the transit model of Riska which, if I understand matters correctly, INSROP proposes to utilize as a part or parts of their routing and economic models. The paper is of considerable interest and is definitely worth publishing.

However, as is usually the case, there are a number of areas where I feel that the paper could be appreciably improved. A detailed listing of these follows:

p.4, paragraph #2 set of preliminary determined routes
predetermined is a better word than preliminary here

p.4, paragraph 3 completely for 35-4o .....85 days
I think that this should say completely over a 35-40 day period etc.

Table 1.1 Giving growth rates without knowing what thicknesses are being referred to is meaningless. This can be corrected by making Table 1.2 the 1st table and then describing the current Rate of Ice Growth Table in terms of the thicknesses given there.

Table 1.2 They say that this table gives Mean multiyear ice thicknesses. This cannot be correct in that many of the thicknesses are < 1 m. Also they say in section 1.1.4 that MY ice thicknesses are >200 cm. Change the caption appropriately.

p. 5, section 1.1.2, 4th paragraph
The way this is worded it reads as if they are describing the boundary between the fast ice and the land which is of course fixed. What they are describing is actually the location of the seaward edge of the fast ice. Change the wording.

Tables 1.3, 1.4, 1.10, 1.11
Several places in the paper the amount of a particular ice type present is described as a % of the area of a sea or a portion of a sea. For this to be useful I would need to know at least the total area of the sea or where the authors consider the boundaries of a particular sea to be located. This information may be given in some other INSROP report. If so it should also be included here for clarity.

Figs. 2.2 and 2.3
There are no units on these graphs

p. 14, 2nd paragraph
I agree with the authors that under certain conditions snow is a very important factor and should not be neglected.

p. 14 last paragraph
A new Russian approach is referred to but it is never described.

p.15, sect. 2.1.4 , 1st paragraph
The Russian National Scale for hummocking should be described. Is it a 4, 6, 8 or 10 scale, etc.

p.16, 1st paragraph
I think that the Riska model uses too many environmental parameters to determine basically only one output, the transit speed. I agree with the authors that you should start model development using the few parameters that are believed to be most important and add items to these later.

p.20, eq (2)
Eq 3 should become 2 and 2 should become 3 as R is a fudge factor in current eq3.

p.22, last paragraph
As the Handbook referred to is not generally available, a description of the floe size scale should be given. For instance if we have floes of scale size 6, does that mean that they are 10 m on diameter or 15 km, etc.

p.23, eq 8
Is this P value the same scale that was referred to earlier??? I would have to see a lot more detail on the use of these floe size relations before I would be convinced that this was describing reality.

p.25 2nd paragraph, last sentence
Personally I do not feel that this criticism of the use of cuttoff values is at all justified.

p.28 line 8
the expression relative are in unit fractions. Does this mean between 0 and 1 instead of a percentage? Clarify this if possible.

Dear Dr. Weeks.

Thank you for your valuable comments, which will allows a significant improvement of the Report under WP2 Project "Natural Conditions along the Selected Routes".

Our answers are in the same order as your questions:

p.4, paragraph 2.
We agree that "predetermined" is a better word than "preliminary".

p.4, paragraph 3.
We have changed the wording.

Table 1.1 serves as a basis for calculating Table 1.2, therefore Table 1.2 cannot be presented as Table 1.1.

Table 1.2.
We agree. The name of the table will be corrected.

p. 5, section 1.1.2, par. 4.
We used an inaccurate term and agree with your correction.

Table 1.3, 1.4, 1.10, 1.11.
We have added a fig. 1.1, showing the boundaries of the regions.

Figs. 2.2 and 2.3.
The figures present the general type (curve type), rather than the precise dependencies. Therefore the units are absent on these graphs.

p. 14, 2nd par.
We agree.

p. 14, last paragraph.
We have included the corresponding reference.

p. 15, section 2.1.4, first paragraph.
We have included a table describing the Russian national scale of hummock and ridge concentration in our report.

p. 16, 1st paragraph.
We agree.

p. 20, eq. 2.
We do not think it is desirable to include in the report a detailed description of transfer from equation 2 to equation 3 as for this it would be necessary to reproduce much of the publication mentioned in the reference before equation 2.

p. 22, last paragraph.
We have made an additional reference to the source, which is generally available.

p. 23, eq. 8
In equation 8, the P value corresponds to the same characteristic as in equations 5 and 6. We have included an additional reference to the publication, which substantiates equation 8.

p. 25, 2nd paragraph, last sentence. The paragraph only states that there are different approaches to investigating ridge height distributions, which have their advantages and disadvantages.

p. 28, line 8.
Yes, the relative area is expressed in unit fractions instead of a percentage. In our opinion, this is the same.

Best regards.
S. Brestkin, A. Yulin

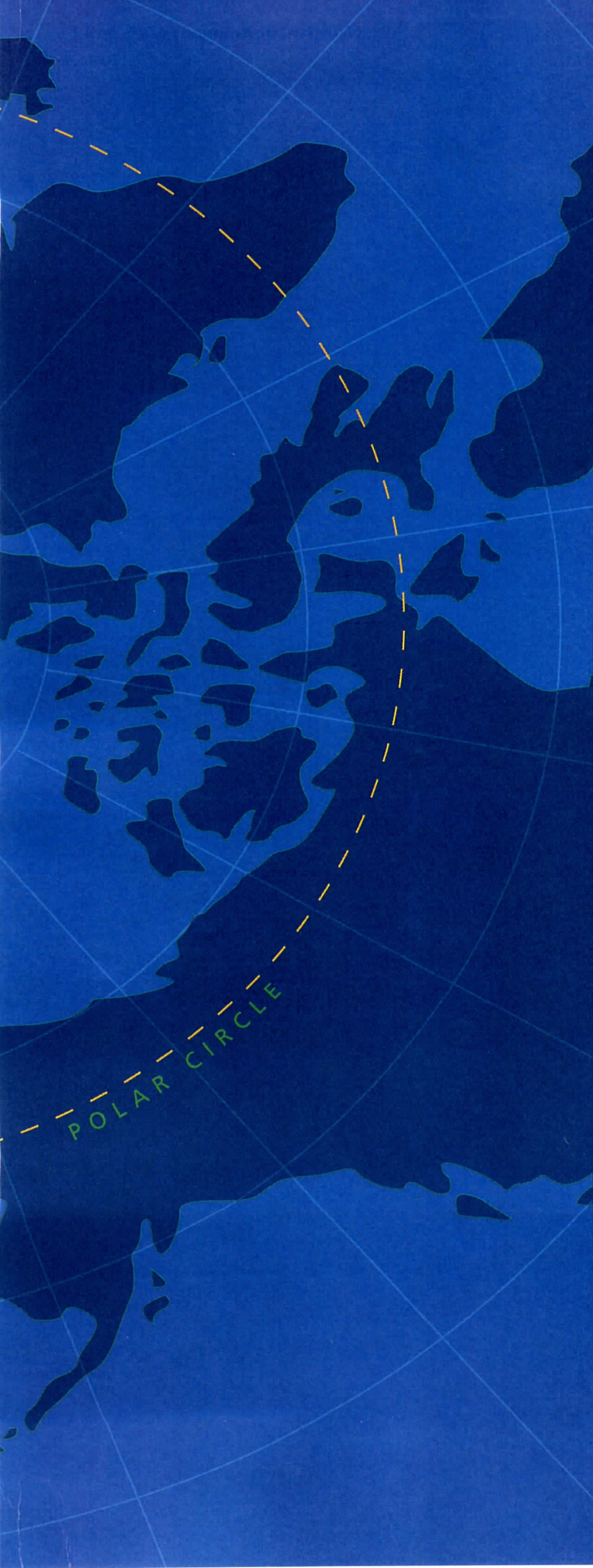

The three main cooperating institutions of INSROP

Ship & Ocean Foundation (SOF), Tokyo, Japan.
SOF was established in 1975 as a non-profit organization to advance modernization and rationalization of Japan's shipbuilding and related industries, and to give assistance to non-profit organizations associated with these industries. SOF is provided with operation funds by the Sasakawa Foundation, the world's largest foundation operated with revenue from motorboat racing. An integral part of SOF, the Tsukuba Institute, carries out experimental research into ocean environment protection and ocean development.

Central Marine Research & Design Institute (CNIIMF), St. Petersburg, Russia.
CNIIMF was founded in 1929. The institute's research focus is applied and technological with four main goals: the improvment of merchant fleet efficiency; shipping safety; technical development of the merchant fleet; and design support for future fleet development. CNIIMF was a Russian state institution up to 1993, when it was converted into a stockholding company.

The Fridtjof Nansen Institute (FNI), Lysaker, Norway.
FNI was founded in 1958 and is based at Polhøgda, the home of Fridtjof Nansen, famous Norwegian polar explorer, scientist, humanist and statesman. The institute spesializes in applied social science research, with special focus on international resource and environmental management. In addition to INSROP, the research is organized in six integrated programmes. Typical of FNI research is a multidisciplinary approach, entailing extensive cooperation with other research institutions both at home and abroad. The INSROP Secretariat is located at FNI.